LUND UNIVERSITY

Modeling time-variant fast fading statistics of mobile peer-to-peer radio channels

Gan, Mingming; Czink, Nicolai; Castiglione, Paolo; Oestges, Claude; Tufvesson, Fredrik; Zemen, Thomas

Link to publication

LUND UNIVERSITY

PO Box 117
221 00 Lund
+46 46-222 00 00

Modeling Time-Variant Fast Fading Statistics of Mobile Peer-to-Peer Radio Channels

Mingming Gan[1], Nicolai Czink[1], Paolo Castiglione[1], Claude Oestges[2], Fredrik Tufvesson[3], Thomas Zemen[1]

[1]FTW Forschungszentrum Telekommunikation Wien, Vienna, Austria
[2]ICTEAM, Université catholique de Louvain, Louvain-la-Neuve, Belgium
[3]Dept. of Electrical and Information Technology, Lund University, Lund, Sweden

Abstract—**The radio channels between nodes of an indoor peer-to-peer network show specific fast fading characteristics. Depending on the mobility and on the scattering properties of the environment, different kinds of fading distributions can occur: Ricean fading between static nodes, but also Rayleigh or even double-Rayleigh fading between mobile nodes.**

We investigate fast fading in indoor peer-to-peer networks based on radio channel measurements. It turns out that the fading statistics change over time. While the predominant fading mechanism is a combination of Rayleigh and double-Rayleigh fading, Ricean fading also occasionally occurs. On top of that, indoors, the *statistics* of the fast fading change over time even for small-motions of the nodes, since the propagation environment is inhomogeneous.

We comprehensively model these effects using a hidden Markov model, parameterized from our measurements. The model is validated, revealing a convincing fit between the model and the measurements.

Keywords—**peer-to-peer channels, fast fading, distributed channel sounding, radio channel modeling.**

I. INTRODUCTION

Cooperative communications is an emerging technology that promises to increase the coverage, reliability and spectral efficiency of peer-to-peer networks [1], [2]. Many methods were introduced, where nodes "help" other nodes to forward their message through the network. Popular schemes are relaying techniques [3], distributed space-time coding [4], or distributed beamforming [5].

The performance of all of these schemes depend on the underlying radio channel. Most of the works on cooperative communications assume Rayleigh fading between the nodes. While this is often true in cellular scenarios, this is not the case in peer-to-peer channels. Here, we observe a strong dependence on the nodes' mobility and on the scattering scenario. For this reason, the peer-to-peer radio channel must be measured and modeled.

The second, and most intriguing motivation for modeling and measuring the peer-to-peer radio channel, is that precise channel characterizations allows the design of cooperative protocols exploiting the specific radio channel properties. For instance, the authors of [6] have shown that cooperative medium access control (MAC) policies for indoor-to-outdoor static networks can capitalize from the knowledge of the Ricean K-factors.

A first thorough investigation of peer-to-peer radio channels in an indoor office environment was carried out in [7], where it turned out that the statistics of small-scale fading may range from strongly Ricean channels (for static nodes) via Rayleigh channels (when only a single node of a link moves) to double-Rayleigh channels (when both nodes of a link move, and rich scattering is present around both nodes).

A further particularity of indoor scenarios is that the statistics of the small-scale fading may change significantly over time for mobile nodes. This is due to the strongly inhomogeneous propagation conditions resulting from the motion of other people, the interaction of the antenna and the user holding the device, and from the fact that the node mobility and the size of obstacles, such as furniture, share a similar geometric scale. Similar observations have been made in [8]. Time-variant fading statistics may be exploited by incentive mechanisms based on repeated games that force nodes to help disadvantaged ones in view of a future exchange of roles, along the lines of [9].

Contribution: In this paper, we analyze and model the variations of the small-scale fading *statistics* based on measurements. We shortly introduce a recent peer-to-peer radio channel measurement campaign carried out in an office environment in Louvain-la-Neuve, Belgium. Based on these experimental results, we evaluate the small-scale fading statistics using the *second-order scattering fading* (SOSF) distribution [10], which reflects any combination of Ricean, Rayleigh, and double-Rayleigh fading [11]. We observe sudden changes of the fading statistics, sometimes with the channel even changing from double-Rayleigh to Ricean.

To model these effects, we introduce a three-step approach: (i) for reflecting the sudden changes of the statistics, we define and parameterize a hidden Markov model [12], (ii) the parameters of the SOSF distribution are modeled according to a β-distribution, fitting the measurements, (iii) fading realizations are generated from the SOSF distribution. After validating our model, we find a convincing fit between the model and the measurements.

This paper is organized as follows: In Section II, we introduce the measurements on which our work is based on. Section III introduces the concept of estimating and modeling time-variant fading statistics, and presents the evaluated model parameters from our measurements. Section IV provides an implementation summary of the model. In Section V, the
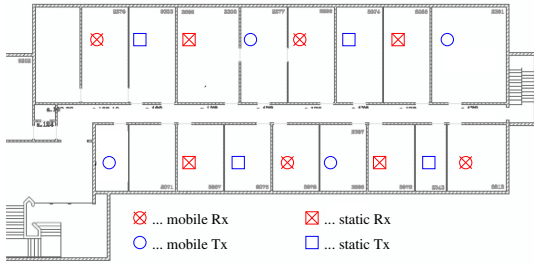
Fig. 1. Floorplan of peer-to-peer measurements

model is validated against measurements. Finally, in Section VI, we draw the conclusions from our work.

II. MEASUREMENTS

A. Environment

Our results are based on indoor peer-to-peer measurements in an office environment. Figure 1 shows a floor plan of the environment. The walls separating the rooms were either brick walls or plaster-board walls. Circles indicate mobile nodes, squares indicate static nodes, and red and blue colors denote receivers (Rx) and transmitters (Tx), respectively. Rx are additionally marked by a cross. The mobile nodes were either randomly moved over a small scale (within a square of $1\,\mathrm{m}^2$), or over a larger scale (throughout the whole room they were in).

Hence, in this environment, we can distinguish between *single-mobile links* (where only one node is moving), *double-mobile links* (where both nodes are moving), and links between static nodes. The statistics of links between static nodes naturally do not change. Hence, this paper only considers links between mobile nodes.

B. Equipment

The measurements were carried out with UCL/ULB Elektrobit CS channel sounder [13] at a carrier frequency of $3.8\,\mathrm{GHz}$, using the switched-array principle. The distributed nodes were connected to the 8-port switches of the transmitter and receiver of the channel sounder using long low-loss RF cables, which had equal length. The RF cables had excellent RF stability, even when they were slightly bent or moved during the measurements. At the nodes, custom-made dipole antennas with a gain of $1.75\,\mathrm{dB}$ and an almost omnidirectional radiation pattern were used.

The channel sounder used long PN sequences to estimate the impulse response of the radio channels between all combination of Tx and Rx nodes. Measurements were done in burst mode, which means that each measurement of the 64 links (8×8 channel) was done four times to increase the SNR by subsequent averaging. The measurement parameters are summarized in Table I. The recorded channel transfer function is denoted by $H[t, f, c]$, where t denotes the time index, f denotes the frequency index, and c denotes the link index.

TABLE I
MEASUREMENT PARAMETERS (AFTER POST-PROCESSING)

Parameter	Value
Carrier frequency	3.8 GHz
Bandwidth	30 MHz
Recorded frequency tones	121
Recorded time samples	300
Measurement duration	113 s

C. Calculating Fast Fading Realizations

Following the concept of [7], the channel can be seen as a superposition of path loss, static shadowing, dynamic shadowing, and fast fading. To extract the fast fading from the channels, we first calculate the average power of the channel in its subbands and use a moving time window as

$$P_s[t, b, c] = \frac{1}{T_{\mathrm{av}} F_{\mathrm{sub}}} \sum_{t'=t-T_{\mathrm{av}}/2}^{t+T_{\mathrm{av}}/2} \sum_{b=1+(b-1)F_{\mathrm{sub}}}^{bF_{\mathrm{sub}}} |H[t', f, c]|^2,$$

where T_{av} denotes the length of the moving time window, and was chosen to be 20 time samples, F_{sub} is the number of freuencies within a subband, and $b = 1 \ldots B$ is the subband index. Subsequently, the realizations of the fast fading are given by

$$G[t, f, c] = \frac{H[t, f, c]}{\sqrt{P_s[t, \lfloor f/F_{\mathrm{sub}} \rfloor, c]}}. \quad (1)$$

III. TIME-VARIANT FAST FADING STATISTICS

A. The SOSF Distribution

Fast fading of peer-to-peer channels can range from being double-Rayleigh to Ricean distributed [7]. A distribution including all these cases is the so-called second-order scattering fading (SOSF) distribution [10]. It describes the distribution of random variables generated by

$$r = |G| = |w_0 e^{j\theta} + w_1 G_1 + w_2 G_2 G_3|, \quad (2)$$

where $G_1, G_2, G_3 \sim \mathcal{CN}(0, 1)$ are complex normal distributed. The factors w_0, w_1, w_2, correspond to the weights of the coherent contribution, single scattering, and double scattering, respectively. It should be noted that w_0 contains all the coherent contributions, not necessarily the line-of-sight path only.

The probability density function of these random variables is given by

$$p_{\mathrm{SOSF}}(r) = r \int_0^\infty \omega e^{-w_1^2 \omega^2/4} \frac{4 J_0(r\omega) J_0(w_0\omega)}{4 + w_2^2 \omega^2} \mathrm{d}\omega, \quad (3)$$

where J_0 is the Bessel function of the first kind and zeroth order. Normalizing the average power as $\mathrm{E}\{r^2\} = 1$, as done in (1), where $\mathrm{E}\{\cdot\}$ denotes the expectation operator, we can introduce the two parameters of the SOSF

$$a = \frac{w_2^2}{w_0^2 + w_1^2 + w_2^2}, \quad (4)$$

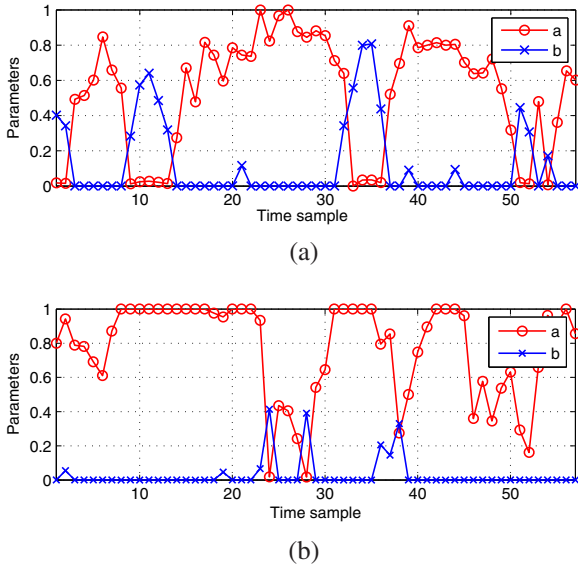$$b = \frac{w_0^2}{w_0^2 + w_1^2 + w_2^2}, \quad (5)$$

Fig. 2. Examples of fast fading distribution parameters over time; (a) single-mobile small-scale motion, (b) double-mobile, large-scale motion.
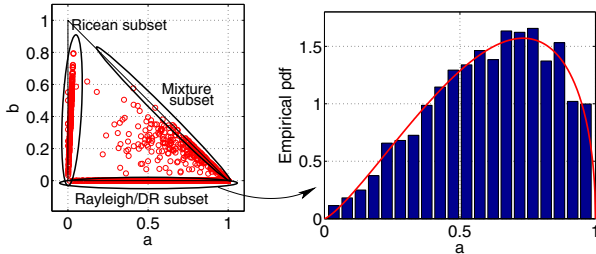

Fig. 3. Parameters of the SOSF exemplary for the single-mobile small-scale motion case. We identify four groups: the Ricean subset, the Rayleigh/double-Rayleigh subset, the Mixture subset, and the pure double-Rayleigh point ($a = 1$, $b = 0$). The distribution within the subsets can be well modeled by the β-distribution, as demonstrated for the Rayleigh/double-Rayleigh subset.

Single mobile, small-scale motion		
Subset	**Probability**	**Distribution**
Ricean	0.11	$b \sim p_\beta(3.0, 4.9)$, $a = 0$
RDR	0.78	$a \sim 0.81 \cdot p_\beta(2.3, 1.5) + 0.19 \cdot \delta(a-1)$, $b = 0$
Mixture	0.12	$\Delta \sim p_\beta(1.4, 7.1)$
Single mobile, large-scale motion		
Subset	**Probability**	**Distribution**
Ricean	0.07	$b \sim p_\beta(2.5, 3.9)$, $a = 0$
RDR	0.8	$a \sim 0.71 \cdot p_\beta(2.6, 1.3) + 0.29 \cdot \delta(a-1)$, $b = 0$
Mixture	0.13	$\Delta \sim p_\beta(2.0, 10.4)$
Double mobile, small-scale motion		
Subset	**Probability**	**Distribution**
RDR	0.85	$a \sim 0.73 \cdot p_\beta(3.1, 1.4) + 0.27 \cdot \delta(a-1)$, $b = 0$
Mixture	0.15	$\Delta \sim p_\beta(1.8, 9.7)$
Double mobile, large-scale motion		
Subset	**Probability**	**Distribution**
RDR	0.88	$a \sim 0.56 \cdot p_\beta(3.0, 1.2) + 0.44 \cdot \delta(a-1)$, $b = 0$
Mixture	0.12	$\Delta \sim p_\beta(1.9, 9.8)$

where a and b are constrained as $a + b \leq 1$, while $a \geq 0$ and $b \geq 0$. The SOSF distribution intrinsically includes Ricean fading (with K-Factor $K = b/(1-b)$, and $a = 0$), Rayleigh fading ($a = b = 0$), and Double-Rayleigh fading ($a = 1$, $b = 0$), but also all combinations of these.

The parameters a and b can be estimated from experimental fading realizations by iteratively fitting the probability density function and/or the cumulative density function, using a moment-based estimate as starting point [10].

As this paper discusses the time variation of the fast fading statistics, our parameters depend on time, leading to $a(t)$, $b(t)$.

B. SOSF Parameters Extracted From Measurements

The variability of the parameters $a(t)$ and $b(t)$ for an exemplary single-mobile channel (with small-scale motion) is investigated in Figure 2a. We mostly observe Rayleigh/double-Rayleigh fading ($0 < a < 1$, $b = 0$). Only scarcely, we observe Ricean fading or a mixture of all fading mechanisms. Looking at a double-mobile channel (with large-scale motion) in Figure 2b, we see that predominantly, double-Rayleigh

fading occurs.

Looking at the statistics of $a(t)$ and $b(t)$ in Figure 3, we observe that their values can be partitioned into four groups: (i) the *Ricean subset* ($a < 0.05$), (ii) the *Rayleigh/double-Rayleigh (RDR) subset* ($0 < a < 1$, $b = 0$), (iii) the *pure double-Rayleigh* case ($a = 1$, $b = 0$), and (iv) the *mixed subset* ($a = 1 - b$). We neglect points in the middle zone, which occur only with a very low probability.

It turns out that the distribution of the parameter b for the Ricean subset can be well approximated by the β-distribution

$$p_\beta(x|p_1, p_2) = \frac{\Gamma(p_1 + p_2)}{\Gamma(p_1)\Gamma(p_2)} x^{p_1-1}(1-x)^{p_2-1}, \quad (6)$$

where $\Gamma(\cdot)$ denotes the Gamma function. For the mixture distribution, we define $\Delta = \sqrt{(1-a)^2 + b^2}$, denoting the points on the line $a = 1 - b$. It turns out that also Δ is β-distributed. Finally, the distribution of the parameter a for the RDR subset can be modeled by a combination of the β-distribution and a Dirac function, combining the mixture of Rayleigh/double-Rayleigh fading and pure double Rayleigh fading, respectively. An example is provided in Figure 3 for the Rayleigh/double-Rayleigh subset (excluding the double-Rayleigh point).

By that we can estimate (i) an overall probability of the subset, and (ii) a probability distribution of the SOSF fading parameters within the subset. A summary of these parameters evaluated from the measurements is provided in Table II. Note that for double-mobile nodes, there were too few samples in the Ricean subset such that it was neglected.

It is noteworthy that we observed a high probability of occurrence for pure double-Rayleigh fading, particularly for double-mobile scenarios.

C. Hidden Markov Model

Modeling transitions between different fading distributions can be solved by using a hidden Markov model (HMM) [12]. Usually in HMMs, the states cannot be directly observed (which coined the attribute "hidden"). However, in our case,

TABLE III
HMM STATE TRANSITION PROBABILITIES

Single mobile, small-scale motion			
from/to	Ricean	RDR	Mixture
Ricean	0.57	0.40	0.03
RDR	0.05	0.85	0.09
Mixture	0.04	0.62	0.33
Single mobile, large-scale motion			
from/to	Ricean	RDR	Mixture
Ricean	0.51	0.40	0.09
RDR	0.04	0.86	0.10
Mixture	0.03	0.61	0.35
Double mobile, small-scale motion			
from/to		RDR	Mixture
RDR		0.88	0.12
Mixture		0.68	0.32
Double mobile, large-scale motion			
from/to		RDR	Mixture
RDR		0.90	0.10
Mixture		0.66	0.34

the parametrization is straightforward, since the underlying distribution can be partitioned into the three cases of fast fading as described above.

Hence, we model the transitions between the subsets using a three-state HMM: (i) Ricean fading, (ii) Rayleigh/double-Rayleigh fading (including pure double-Rayleigh fading), and (iii) mixed fading.

The state transition probabilities were estimated from the measurements and are presented in Table III for the four cases. The validity of the Markov chain was verified by testing that all state transitions only depend on the current state and are uncorrelated with previous states.

IV. MODEL SUMMARY

Summarizing, we propose to model small-scale fading with time-variant statistics as shown in Figure 4. We start with a random initial state of the HMM. Depending on the state, we draw the SOSF parameters (a, b) from the distributions provided in Table II. Using (a, b), we generate a pre-defined number of complex fading realizations G using (2) and (4),(5).

Next, the state of the HMM is updated. If the state changes, we draw new SOSF parameters and continue with generating fading realizations. If the state is unchanged, we skip drawing new SOSF parameters. This simplification turns out to have no noticeable impact on the distribution and helps to keep the model simple.

V. VALIDATION

To validate the model, we investigate the overall fit to measurement data. For that, we generated realizations with time-variant statistics using the model in Section IV.

Figure 5 compares the cumulative distribution function (CDF) of the generated fast-fading samples of the single-mobile measurements (dotted line) and of the model (solid line), for both large-scale motion (bold line, blue color) and small-scale motion (thin line, red color). It is evident that the distributions fit very well. Interestingly, there is no significant
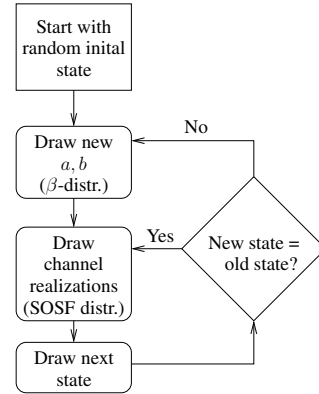

Fig. 4. Flow diagram of the model, generating fast fading realization with time-variant statistics
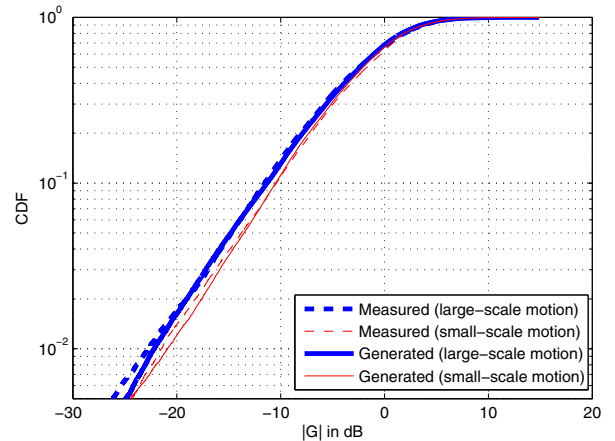

Fig. 5. Fit of the model to measurement data: empirical CDF of the fading realizations evaluated from the measurement data (single mobile, small-scale and large-scale motion), and from the generated channels.

difference between large-scale and small-scale motion in the overall CDF in this scenario[1].

Comparing the measurements with the conventional Rayleigh, Ricean, and double-Rayleigh distributions, we observe from Figure 6 that none of these distributions reasonably fit the experimental data.

It must be noted that this validation only tells whether the overall statistics are reflected correctly. They do not tell, whether the transition between the different fading statistics are captured correctly. However, this aspect was covered by validating the HMM as described in Section III-C.

VI. CONCLUSIONS

This paper has presented an empirical model of *time-variant* fading statistics of a peer-to-peer network in an indoor office environment. The measured data is characterized by the second-order scattering fading distribution (SOSF) [10],

---

[1]Note that, regardless of small-scale or large-scale *motion*, only the *fast fading* distribution is evaluated here, which must not be mixed with the large-scale fading or shadow fading.
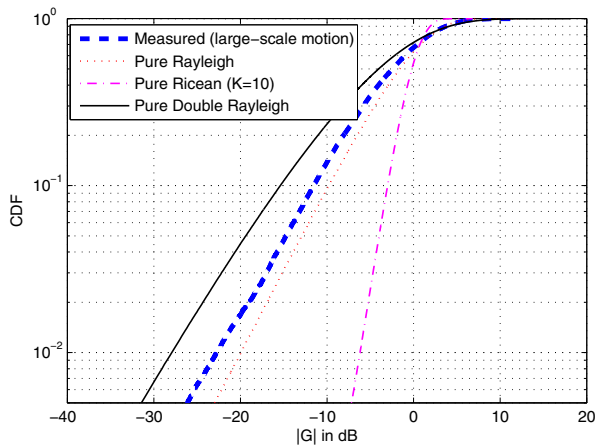
Fig. 6. Comparison with conventional fast-fading distributions

which is able to model all varieties of fast fading from double-Rayleigh to Ricean. The parameters of the SOSF can be partitioned in three groups: Ricean fading, Rayleigh/double-Rayleigh fading, and a mixture of these. The probabilities of occurrence (and parameters of the SOSF) in these groups depend on the scenario, particularly on the mobility of the nodes. Transitions between the groups are described by a hidden Markov model.

The simulations show that our model represents the measured distributions correctly. Interestingly, the fast fading distributions for large-scale and small-scale motions of the nodes are quite similar. Particularly, we also observe pure double-Rayleigh fading which is specific to a rich-scattering peer-to-peer environment.

REFERENCES

[1] A. Sendonaris, E. Erkip, and B. Aazhang, "User cooperation diversity. Part I: System description," *IEEE Trans. Commun.*, vol. 51, no. 11, pp. 1927–1938, Nov. 2003.

[2] ——, "User cooperation diversity. Part II: Implementation aspects and performance analysis," *IEEE Trans. Commun.*, vol. 51, no. 11, pp. 1939–1948, Nov. 2003.

[3] R. Nabar, H. Boelcskei, and F. Kneubuehler, "Fading relay channels: performance limits and space-time signal design," *IEEE J. Select. Areas Commun.*, vol. 22, no. 6, pp. 1099–1109, Aug 2004.

[4] J. Laneman and G. Wornell, "Distributed space-time-coded protocols for exploiting cooperative diversity in wireless networks," *IEEE Trans. Inform. Theory*, vol. 49, no. 10, pp. 2415–2425, Oct. 2003.

[5] H. Ochiai, P. Mitran, H. Poor, and V. Tarokh, "Collaborative beamforming for distributed wireless ad hoc sensor networks," *IEEE Trans. Signal Processing*, vol. 53, no. 11, pp. 4110–4124, Nov. 2005.

[6] P. Castiglione, S. Savazzi, M. Nicoli, and T. Zemen, "Impact of fading statistics on partner selection in indoor-to-outdoor cooperative networks," in *IEEE International Conference on Communications (ICC)*, Cape Town, South Africa, May 23-27 2010.

[7] C. Oestges, N. Czink, B. Bandemer, P. Castiglione, F. Kaltenberger, and A. Paulraj, "Experimental characterization and modeling of outdoor-to-indoor and indoor-to-indoor distributed channels," *IEEE Transactions on Vehicular Technology*, vol. 59, no. 5, pp. 2253–2265, jun. 2010.

[8] J. Karedal, A. J. Johansson, F. Tufvesson, and A. Molisch, "A measurement-based fading model for wireless personal area networks," *IEEE Trans. Wireless Commun.*, vol. 7, no. 11, pp. 4575–4585, 2008.

[9] M. Le Treust and S. Lasaulce, "A repeated game formulation of energy-efficient decentralized power control," *to appear in IEEE Transactions on Wireless Comm.*, 2010.

[10] B. Bandemer, C. Oestges, N. Czink, and A. Paulraj, "Physically motivated fast-fading model for indoor peer-to-peer channels," *Electronics Letters*, vol. 45, no. 10, pp. 515–517, 7 2009.

[11] C. Oestges and B. Clerckx, *MIMO Wireless Communications*. Elsevier Academic Press, 2007.

[12] Y. Ephraim and N. Merhav, "Hidden markov processes," *Information Theory, IEEE Transactions on*, vol. 48, no. 6, pp. 1518–1569, jun. 2002.

[13] Elektrobit EB Propsim Homepage, 2008. [Online]. Available: http://www.propsim.com